Chapter 2

NLC Parameters and Layout

2.1 Introduction

Over the last five years, the physics program for a linear collider has evolved significantly [1], and as a consequence, the layout of the NLC has been modified to provide greater energy flexibility. Recent precision measurements of electroweak parameters provide a convincing case that some new physics to explain the mechanism of electroweak symmetry breaking will be seen at energies of 0.5 to 1.0 TeV. A linear collider in this energy range will be able to make precision measurements to complement the results from the Tevatron and LHC. In addition, there is considerable interest in precision measurements at lower energies, such as the Z^0, W-pair, or Top thresholds. The physics scenarios considered also indicate that the collider should eventually be able to support an upgrade to multi-TeV energies, once a suitable rf technology can be developed. This is discussed further in section 2.4.

The NLC was presented in detail in the 1996 *Zeroth-Order Design Report for the NLC* (ZDR) [2]. During the last five years, the linear collider R&D program has led to substantial improvements in that design. As described in the previous chapter, the NLC design is based on extensive experience from the first linear collider, the SLC, as well as other modern accelerators, and from numerous test facilities including ASSET, FFTB and NLCTA at SLAC and the ATF at KEK. These are described briefly in Chapter 1 and in more detail in later chapters. The polarized electron source and the positron production system are modest extensions of the SLC sources. The damping rings are similar to third-generation synchrotron light sources and are required to produce an equilibrium emittance that is only a factor of two below what has been achieved at the ALS in Berkeley or the ATF. A prototype X-band rf system has been operated successfully at the NLCTA since 1996. In principal, this system could be used today to build a 500-GeV cms collider, but there is active R&D on a next generation of components that are more efficient and less expensive to build and operate.

To preserve the small beam emittance during acceleration, the X-band structures must be designed to minimize wakefields, and both the structures and the focusing quadrupoles must be aligned to very tight tolerances. The wakefield properties of prototype structures have been measured precisely in the ASSET test facility and agree well with the calculations [3]. Structures have been fabricated which meet tolerances far tighter than those required for NLC. The required alignment accuracy has also been demonstrated in ASSET. Beam-based alignment techniques developed for the SLC and FFTB have achieved close to the necessary accuracy, and extensive simulations indicate that these techniques are capable of preserving the emittance through a 10- km linac with diagnostics and correction hardware which need to be only a factor of 3 to 5 better than those used at the FFTB. The FFTB also demonstrated the validity of the final-focus optics and achieved a demagnification of the beam size greater than required for NLC. All of these results have led to improvements in the design and increased confidence in its capabilities.

Together with the accelerator hardware and optics, the beam parameters and the NLC collider layout have evolved since the 1996 design. These changes have been motivated by a desire to provide additional physics functionality and to reduce the capital costs of the facility. A schematic of the NLC is shown in the previous chapter in Fig. 1.1. The collider is roughly 30 km in length. It consists of two 13-km-long X-band linacs that will accelerate the beams to 500 GeV for collisions at 1 TeV in the center-of -mass. In addition to the linacs, there are electron and positron injector complexes and a beam-delivery system that supports two interaction regions. The collider is intended to begin operation at a center-of-mass energy of 500 GeV, in which case the linac tunnels would only be half filled with accelerator structures and rf power sources. In addition, there are bypass lines to deliver low-energy beam to either IR as desired.

In the following sections, the collider layout is discussed in more detail. The beam and IP parameters are described in section 2.2. The last sections cover further options for additional functionality and possible routes to a multi-TeV facility.

2.2 Layout

The layout of the linear collider is described starting first with the final focus and interaction regions, and following with the main linacs and injector systems.

2.2.1 Final Focus and Interaction Regions

Given sufficient acceleration to produce a beam of the desired energy, a major limitation on the energy range of a linear collider is the final-focus system. In order to cancel the chromaticity of the final quadrupoles that focus the beams to the necessary small size at the interaction point (IP), the final-focus optics include pairs of sextupoles separated by bending magnets. The bends must be weak to avoid emittance dilution from synchrotron radiation. Because of this, the magnets must be long, and their length determines the overall length of the final focus. For a given optics design, the strength of the bends also limits the maximum energy beam that can be delivered without excessive emittance growth. A linear-collider final focus can typically span a factor of 4 in energy. Over this range, the luminosity increases linearly with energy as the beam emittance shrinks through adiabatic damping. Above the maximum design energy, the luminosity falls due to emittance dilution from synchrotron radiation in the bends. Below the minimum design energy, the luminosity is usually proportional to the square of the beam energy because apertures and aberrations in the collimation or final-focus regions limit the achievable demagnification at the IP.

To accommodate the physics demand for energy flexibility, the NLC design now includes two interaction regions. One is optimized for high energy, 250 GeV to 1 TeV, and is configured so that it is ultimately upgradeable to multi-TeV. The other is designed for precision measurements at lower energy, 90 to 500 GeV. The luminosity for each IR increases linearly with energy over the design energy range as shown in Fig. 2.1. This configuration was inspired by a breakthrough in the final-focus optics design that made the system much more compact [4]. By interleaving the chromatic correction sextupoles with the final quadrupoles, fewer long bending magnets are required. The new optics are described in more detail in Chapter 6. With this design, the final focus can accommodate beams of up to 2.5 TeV in a length of about 800 meters. By comparison, a conventional design for the CLIC final focus is 3-km long for 1.5-TeV beams.

To capitalize on the multi-TeV potential of the new design, it was also necessary to eliminate other bending between the linac and the high energy IP. In the NLC design, a 20-mrad crossing angle at the IP is needed to avoid parasitic interactions of one bunch with the later bunches in the opposing train. The earlier NLC design had two symmetrically placed interaction regions (IR) with a ‘Big Bend’ to separate the beams and generate this crossing angle. To reduce synchrotron-radiation emittance growth, the Big Bend was long (and expensive) and ultimately limited the maximum beam energy. In the new asymmetric layout, the linacs are no longer collinear but are oriented with a shallow 20-mrad angle between them to produce the desired crossing angle at the high-energy IR without additional bending. The beams to the second IR are bent by about 25 mrad, which is acceptable because they are at lower energy. This allows reasonable luminosity up to 1 TeV. The low-energy IR has a larger 30-mrad crossing angle for compatibility with a possible $\gamma\gamma$ option which is described in Chapter 8.

The beam line for the high energy IR is 2.5 km from the end of the linac. This distance includes a long 1.4-km collimation region, the 800-m final focus and an additional 300 m ‘stretch’ to accommodate the beamlines for the low-energy IR. The low-energy IR beam line splits off at the end of the collimation region and includes the 25-mrad bend and a shorter 500-m final focus. Both beam lines share the same collimation system but, as a future upgrade, parallel collimator beam lines could be installed in the same tunnel. An alternate configuration with separate beam lines from the end of the linac to the two IRs is possible, but the extra tunnel length makes it more costly. In the present layout, the two IRs are separated by about 20 m transversely and 440 m longitudinally to provide vibration isolation and shielding so either IR hall may be accessed while the other is in operation.

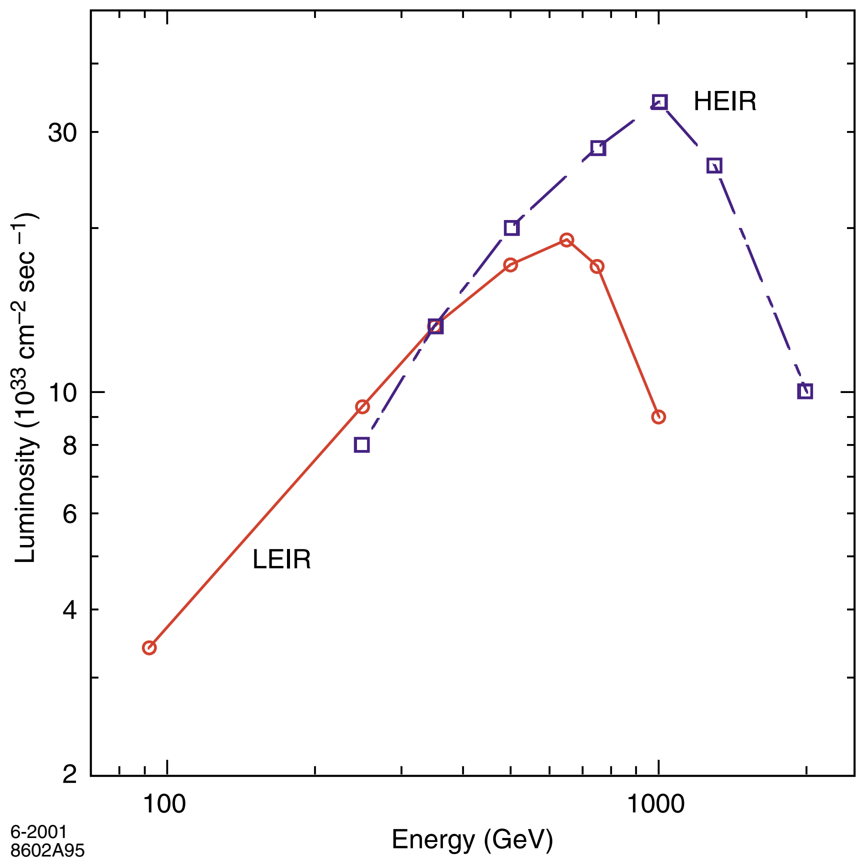

Figure 2.1: Luminosity as a function of energy for the high and low energy IRs.

2.2.2 Main Linacs

The main-linac rf system has been outlined in Chapter 1 and will be described in detail in Chapter 4. Each linac consists of 26 rf sectors which are 468-meters long. The rf power is generated in modulator/klystron '8-packs' where one solid-state modulator drives 8 attached klystrons. Each sector is powered by nine of these 8-packs that feed the rf distribution waveguide. The 8-packs would not be installed in the main linac tunnel but in a separate enclosure. This simplifies access and maintenance, and it is essential to ensure the desired reliability and collider availability.

The main-linac tunnels are designed to be long enough to hold the full complement of accelerating structures in the 26 sectors required to reach 500 GeV per beam. The tunnels are roughly 12.8 km in length. In the first stage of the project, only the first 13 sectors - half the tunnel length - would be filled with structures. The installation would start from the low-energy end of the tunnel to allow maximum flexibility in choosing the appropriate energy upgrade steps to match physics interest and funding profiles.

Because of the transverse wakefields of the accelerator structures, it is undesirable to transport the beam through a large number of unpowered structures. In order to maximize luminosity at lower energy, a nonaccelerating 'bypass' line is provided to bring the low-energy beams to the end of the linac. This system is similar to that used for PEP-II injection at SLAC. The bypass line will share the main-linac tunnel, and will be installed at the same elevation as the main beam line. The design includes three transfer points where the beam can be diverted into the bypass line at 50, 150 and 250 GeV, and a return at the end of the linac to bring the beam back into the collimation section. These are sufficient to support a continuous variation of beam energy over the whole range. The bypass line will also be used to transport the beam from the end of the installed rf to the end of the linac, eliminating the need to provide a drift tube and focusing magnets in the unfilled part of the main-linac beam line.

In addition, there will be four diagnostic regions along the length of the linac where the beam emittance and the beam energy and energy spread can be monitored parasitically. Continuous, noninvasive monitoring was found to be essential during the SLC operation because it facilitates rapid diagnosis of faults and makes it possible to correlate disparate effects. The bypass line injection and extraction regions and special nonaccelerating diagnostic regions increase the linac tunnel length by roughly 500 m.

2.2.3 Injector Systems

There are two separate injector complexes to produce the low-emittance trains of electron and positron bunches for injection into the main linac. Each train consists of 190 bunches of 0.75×10^{10} particles per bunch, separated by 1.4 ns. The electrons have 80% polarization and the positrons are unpolarized. The electron injector includes a polarized photocathode gun, a bunching system and an S-band booster linac to deliver 1.98-GeV beam to the damping ring. For the positron injector, an unpolarized electron gun and bunching system followed by a 6-GeV drive linac provides the electron beam needed to produce positrons. Multiple positron targets are required to keep the energy deposited in each target below the threshold for material damage. The electrons are split by an rf separator and directed onto 3 of 4 multiplexed targets and positron capture sections. The bunches are then recombined into the desired 190-bunch train format and accelerated in a 1.98-GeV L-band linac to the positron predamping ring. Because of the large emittance of the captured positrons, large-aperture L-band rf is used for acceleration and a predamping ring is required to reduce the emittance of the positrons before injection into the main damping ring. Two identical rings are used to damp the positron and electron bunch trains from the injectors to a normalized emittance of 3×10^{-6} m-rad in the horizontal and 2×10^{-8} m-rad in the vertical.

After extraction from the damping rings, the beam passes through a spin rotator system that can be used to orient the electron spin in an arbitrary direction to ensure longitudinal polarization of the beams at the IP. In the baseline design, the spin rotating solenoids are only installed in the electron beam line. However, the positron beam line is identical so that additional solenoids can easily be installed later. This would allow operation either with polarized positrons or with polarized electrons for $\gamma\gamma$ or e^-e^- collisions.

After the spin rotators, the bunch length must be compressed from 4 mm to 110 μm before injection into the main X-band linacs. This is accomplished in a 2-stage bunch compressor that is identical for the two beams. The first stage uses an L-band rf section followed by a wiggler to compress the bunch to a length of about 0.5 mm. This is followed by a 6-GeV S-band prelinac and the second-stage bunch compressor with a 180° arc, an X-band rf section and a chicane. The second stage can produce a bunch length between 90 and 150 μm. The NLC injector complexes are described in detail in Chapter 5. In the present layout, the electron booster and prelinac are housed in the same tunnel to minimize infrastructure costs. The positron drive linac, booster and prelinacs also share a common tunnel and support buildings.

The concept of a central injector complex was investigated for possible cost savings, and many configurations with and without shared components were considered. Any centralized injector requires long, low-emittance transport lines to bring the beams to the end of the main linacs and extra tunnels to connect into the linac housing and into the second bunch-compressor 180° turnaround. These additions more than offset any potential savings. The most cost-effective location for the injectors is near the low-energy ends of the linacs as in the original ZDR design. A central injector design is being developed for the Fermilab deep-tunnel site because it has the advantage of being located entirely on land already owned by the laboratory.

2.3 Parameters and Luminosity Evolution

The primary parameters for the NLC are listed in Table 2.1. The beams consist of bunch trains with 190 bunches separated by 1.4 ns at a repetition rate of 120 Hz. During the initial stage the center-of-mass energy is assumed to be 500 GeV with a luminosity of 2.0×10^{34} cm^{-2}s^{-1}, although the collider might be started with a lower initial energy depending on the physics interest. The second stage assumes the installation of the full rf system to reach a center-of-mass energy of 1 TeV with a luminosity of 3.4×10^{34} cm^{-2}s^{-1}. Using the bypass lines and the two interaction regions, the collider is designed to cover fully the energy range between 90 GeV and 1 TeV cms. Sets of nominal parameters for operation of the low-energy IR are listed in Table 2.2. The operating energy ranges of the two interaction regions were discussed in the previous section.

The beam parameters listed in Tables 2.1 and 2.2 have been chosen to optimize the fraction of luminosity close to the center-of-mass energy and minimize the beamstrahlung-related backgrounds. The beamstrahlung can be described by two parameters, the number of beamstrahlung photons radiated per incident electron n_γ and the average energy lost to the beamstrahlung δ_B. In general, the luminosity close to the center-of-mass energy depends most sensitively on the total number of photons radiated while the tails of the luminosity distribution are described by the average energy lost. The number of hadronic background events is proportional to the square of the total number of photons and is a function of the photon energy spectrum. The number of photons depends on the ratio of the number of particles per bunch and the horizontal beam size while the beamstrahlung energy loss has a similar dependence but is also a function of the bunch length. These parameters can be traded against each other to optimize the total luminosity and the luminosity spectrum for any given experiment. The parameters presented in Tables 2.1 and 2.2 are only an illustrative set.

Since the NLC 1-TeV parameters have evolved significantly since the 1996 ZDR [2], it is worth describing those changes in detail. First, the unloaded acceleration gradient has been decreased from 85 MV/m to 70 MV/m. This reduced the rf power required in the accelerator structures, and is close to the cost optimum for the linac. Second, there have been two major changes to the bunch-train format: the single bunch charge and bunch length have decreased by 30%, reducing the average beam current and the beam loading; and the bunch train length and the number of bunches in the train have doubled, increasing the rf-to-beam efficiency and recovering the luminosity lost due to the decrease in the single bunch charge.

The decrease in the bunch charge and the average current then has three effects: (1) it reduces the capital costs because the beam loading is lower and thus, for the same unloaded gradient, the length of the linac is shorter to produce the same final energy; (2) it allows for shorter bunch lengths because the effects of the longitudinal wakefields are smaller; and (3) it reduces the emittance dilution from the transverse wakefields. In the NLC, the alignment tolerances are dominated by single bunch effects. By reducing the product of the charge and the bunch length from $1.1 \times 10^{10} \times 150$ μm to $0.75 \times 10^{10} \times 110$ μm, the expected emittance dilution due to transverse wakefields is reduced by a factor of four. The emittance dilution due to quadrupole misalignments will also be reduced by a comparable factor because the dominant dilution arises from the energy spread needed for 'BNS damping' (see section 7.4.1), which is proportional to the transverse wakefield.

These changes, along with expected performance improvements from the hardware, have led to a decrease in the emittance dilution budgets. This allows operating parameters with smaller beam sizes at

Table 2.1: Parameters for Stage 1 and Stage 2 of the NLC

PARAMETER NAME	**STAGE 1**	**STAGE 2**
CMS Energy (GeV)	500	1000
Luminosity (10^{33}) inc. dilutions	20	34
Luminosity within 1% of E_{cms} (%)	55	44
Repetition Rate (Hz)	120	120
Bunch Charge (10^{10})	0.75	0.75
Bunches/Rf Pulse	190	190
Bunch Separation (ns)	1.4	1.4
Eff. Gradient (MV/m)	48	48
Lum. Dilution for tuning and jitter (%)	10	10
Injected $\gamma\varepsilon_x$ / $\gamma\varepsilon_y$ (10^{-8} m-rad)	300 / 2	300 / 2
$\gamma\varepsilon_x$ / $\gamma\varepsilon_y$ at IP (10^{-8} m-rad)	360 / 3.5	360 / 3.5
β_x / β_y at IP (mm)	8 / 0.10	10 / 0.12
σ_x / σ_y at IP (nm)	245 / 2.7	190 / 2.1
σ_z at IP (μm)	110	110
Υ_{ave}	0.11	0.29
Pinch Enhancement	1.43	1.49
Beamstrahlung δ_B (%)	4.7	10.2
Photons per e^+/e^-: n_γ	1.2	1.3
Linac Length (km)	6.3	12.8

Table 2.2: Low energy operation parameters for the NLC

Energy (GeV cms)	**92**	**250**	**350**
Luminosity (10^{33})	3.5	9.4	13.2
Luminosity within 1% of E_{cms} (%)	92	75	65
Repetition Rate (Hz)	120	120	120
Bunch Charge (10^{10})	0.75	0.75	0.75
σ_x / σ_y at IP (nm)	630 / 6.2	380 / 3.8	320 / 3.2
Beamstrahlung δ_B (%)	0.18	1.1	2
Photons per e^+/e^-: n_γ	0.49	0.79	0.92
Polarization loss (%)	0.08	0.21	0.34

the IP and improved luminosity performance. The changes are summarized in Table 2.3, which compares parameters for the NLC ZDR and the present design at 1 TeV in the center-of-mass. In particular, the luminosity at 1 TeV has more than tripled but, because of the changes in the bunch-train format, the tolerances on the beam line components have only decreased by 30%. To attain these tolerances, beam-based alignment techniques are necessary. The performance of these beam-based algorithms depends primarily upon the precision of the beam diagnostics and corrections. As will be discussed in Chapter 7, the R&D program has demonstrated that the diagnostics will have much better performance than was expected at the time the ZDR was written.

Table 2.3: Parameters for 1996 and 2001 NLC designs at 1 TeV

PARAMETER NAME	NLC ZDR (1996)	NLC 2001
Bunch charge	1.1×10^{10}	0.75×10^{10}
Bunch length	150 μm	110 μm
Bunch train format	75 bunches separated by 1.4 ns	190 bunches separated by 1.4 ns
Unloaded acc. gradient	85 MV/m	70 MV/m
Active linac length	8.8 km	10.1 km
Luminosity	1.1×10^{34} cm^{-2}sec^{-1}	3.4×10^{34} cm^{-2}sec^{-1}
Dilution for jitter and tuning	16 %	10 %
σ_x and σ_y at IP	250×4.1 nm	190×2.1 nm
Alignment tolerance	12 μm rms	9 μm rms

Detailed budgets for emittance dilution and beam jitter have been developed for the NLC. These are given in Chapter 7 along with a discussion of the beam-based alignment and jitter-stabilization techniques. The design luminosities, listed in Table 2.1, include an estimated 10% luminosity degradation beyond the explicit emittance dilutions to account for beam jitter and beam tuning. This tuning estimate is based on the results of the SLC 'dither-tuning feedback' [5] which very effectively optimized the linear optics automatically by using heavily averaged signals proportional to the luminosity. This technique was developed in the last year of SLC operation, and proved much more effective than the methods assumed in 1996.

Table 2.4: Intrinsic versus design emittances and luminosity for NLC at 1 TeV

	INTRINSIC x/y	DESIGN x/y
Damping Ring Emittance (10^{-8} m-rad)	300 / 1	300 / 2
Main Linac Emittance (10^{-8} m-rad)	315 / 1	330 / 3
Beam Delivery Emittance (10^{-8} m-rad)	330 / 1	360 / 3.5
Luminosity (cm^{-2}sec^{-1})	6.6×10^{34}	3.4×10^{34}

Finally, it should be noted that the ultimate luminosity of the collider is roughly a factor of two higher than the design. This might be attained if the beam-based alignment techniques can be pushed to even higher precision. The ultimate luminosity, referred to as 'intrinsic luminosity,' is determined by physical limitations such as the finite damping time of the damping rings and synchrotron-radiation emission in the bunch compressors and final focus. These intrinsic beam emittances and luminosity are listed in Table 2.4 for comparison with the design values.

2.4 Options Beyond the Baseline Design

There are a number of options that have been considered to extend the physics reach of the NLC beyond what has been described as the baseline design. These include:

- Simultaneous delivery of luminosity to the two interaction regions
- Higher repetition rate for the low-energy portion of the linac to increase the total luminosity delivered.
- Operation in e^-e^-, $e^-\gamma$, and $\gamma\gamma$ modes
- Operation with polarized positrons.

Finally, while the primary purpose of the NLC linear collider lies in studies of high-energy physics in the sub-TeV to TeV energy range, the availability of ultra-low emittance, high-energy electron and positron beams could provide opportunities for research in other branches of science:

- Low-emittance, high-energy electron and positron beams extracted at various points in the linear-collider facility could be used for fixed-target experiments for either high-energy or nuclear physics. Either the incident particle beam or a high-energy photon beam could be available.
- High-energy particle beams can be used to generate low-current test beams to verify detector components or for other special experiments
- Low-emittance, short bunches of electrons at high energies, with suitably low energy spread, could be used to drive a Free Electron Laser.

In this section, we summarize briefly some considerations and issues concerning these options for the NLC.

2.4.1 Simultaneous Operation and 180 Hz

With an interaction region dedicated for precision low-energy measurements and bypass lines for the low-energy beams in the linac, two additional options have been considered to broaden the NLC physics program for a modest increase in cost. These are the possibility of simultaneous operation of both IRs with interleaved pulses, and the possibility of higher repetition rate for the low-energy beams. The basic operating model for all of the linear-collider designs has been to deliver beam to only one IR before switching to the other IR. With simultaneous operation, the entire bunch train would be sent to one detector or the other on a pulse-by-pulse basis and both detectors could record data at once. The bypass lines, if pulsed, would make it possible for the two detectors to operate with beams of different energy. The only significant addition required for operation with two energies would be a separate collimation system for the second energy beam. In the present layout, the two collimator lines would share the same tunnel. For simultaneous operation, one also needs to orient the electron polarization appropriately so that it is longitudinal at each IP. This is believed to be a solvable problem although it has not yet been studied in detail.

At a fixed repetition rate, the simultaneous operation described above does not increase the total luminosity but simply splits it between the experiments. The concept becomes much more attractive if the low-energy part of the collider could be run at 180 Hz with the rate shared between IRs at either 120/60 or 90/90 Hz. Most of the injector components could easily be designed to support the additional load of 180-Hz operation. The key technical challenges are the damping rings and the cooling for the X-band klystrons. In the present ring design, the damping time is insufficient at 180 Hz. An alternative possibility with two 90-Hz damping rings in a common vault has been studied and appears feasible. These rings could be 200 m in circumference instead of 300 m for the present ring, but would still require a large number of additional components at increased cost. Adequate cooling is already an issue for the periodic permanent magnet (PPM) focused X-band klystrons because of the small dimensions of the magnet assembly. More R&D would be required to demonstrate sufficient cooling for 180-Hz operation. Finally, it should be noted that the fractional increase in total ac power to the collider site is small for the higher repetition rate. For some choices of rates and beam energies, no additional site power would be required.

For the present, neither option is mature enough to be included in the NLC design, but both are attractive enough to warrant further study. As far as possible the configuration of the machine has been chosen to maintain compatibility with both options as future upgrades.

2.4.2 Alternate Collision Options: $\gamma\gamma$, e^-e^-, $e^-\gamma$

Several alternate types of collisions have been proposed for the collider because they access new physics channels or offer additional types of measurements. These include collisions of polarized photons ($\gamma\gamma$), polarized electrons (e^-e^-), electrons on photons ($e^-\gamma$) and polarized positrons on electrons. A number of workshops have been dedicated to these issues and discussions can be found in references [5] and [6].

Of the first three, the $\gamma\gamma$ option has elicited the strongest interest. Recent progress on a high-powered laser system to produce the photons has greatly enhanced the viability of this option and it is discussed further in Chapter 8. The NLC design includes a larger crossing angle for the low-energy IR to accommodate the larger size of the disrupted beam from $\gamma\gamma$ collisions.

To transport polarized beams through the damping-ring complex, a system of spin rotators is required before and after the rings. These are included in the design for the electron injector, and space has been reserved in the positron complex to allow them to be installed later, if required for either polarized positrons or a second polarized electron beam. The positron injector also provides a beam line to transport the drive electrons directly to the damping ring, bypassing the positron production system, as needed for any of the γ or e^- options.

2.4.3 Positron polarization

Polarized positrons can be important for certain precision measurements and would be crucial to reduce systematics for a 'Giga-Z' run. A polarized positron beam for a linear collider can be created by pair conversion of polarized photons produced either from an undulator or by Compton scattering off a high-power laser. The R&D on both of these options is discussed in Chapter 5.

2.4.4 Use of Extracted Beams

The high-energy beams generated by the main accelerators would likely have a number of uses other than the primary physics experiments. For example, it is almost certain that a facility would be needed for generating very-low-current test beams with close to the full beam energy. These could be produced by capturing some of the particles in the beam halo and then redirecting them to an alternate beam line. The best location for these test beams will depend on the proposed utilization.

In addition, the high-energy beams from the NLC can be used to generate a very-high-intensity photon beam for nuclear physics and other applications. For example, photons of energies from 2 to 50 MeV can be produced with electron beams of energies from 50 to 250 GeV. A 100-m-long undulator would produce roughly $1\text{x}10^{11}$ photons per bunch, or $2\text{x}10^{13}$ per train. For the 250-GeV case, this corresponds to an average power of ~75 kW in the photon beam. The output of the undulator can be collimated to produce a narrow spectrum (limited by the 0.3% energy spread of the electron beam). There will be $\sim10^{10}$ photons per pulse ($\sim10^{14}$ per second) in this energy width in a ~500-micron beam with a sub-microradian divergence angle. The photon beam could be produced either by a dedicated beam or parasitically by the primary beam headed towards the interaction regions. In the latter case, the undulator would have to be installed in the linac tunnel.

Finally, the primary beams could also be used for dedicated fixed-target experiments. They would have five times more energy and two times higher average current than the highest-current SLAC end-station experiments. This would allow, for example, a Möller scattering measurement of the weak mixing angle at higher Q^2 than the E-158 experiment at SLAC. There are a number of possible locations where the end station of NLC might be located downstream of the interaction point. When the beams are not in collision, a high-brightness beam could be transmitted through the NLC IR to the end station. If fixed-target positron experiments are desired, a second end station could be constructed on the positron dump line.

2.4.5 Possible Implementations of the FEL Subsystems at the NLC

A coherent pulse of X-rays can be generated by a Free Electron Laser (FEL). Because highly reflective mirrors are difficult at short wavelengths, most X-ray FELs are based on the Stimulated Amplification of Spontaneous Emission (SASE) concept. With SASE, a high-current, low-emittance electron beam is passed through a long undulator and the spontaneous radiation at the resonant wavelength is amplified. The concept of a SASE-based X-ray Free Electron Laser (FEL) has been studied at SLAC using the SLAC linac [8]. This is now the basis of a formal proposal, the Linac Coherent Light Source (LCLS) [9], which is expected to begin construction in 2004.

The idea of introducing an X-ray FEL into the linear collider facility is discussed extensively in the TESLA TDR. For the NLC, this option has not been strongly pursued because the advantages of integrating this facility into the collider are not yet clear. The FEL requires electron beams of between 15 and 50 GeV. Unfortunately, the desired beam emittance and longitudinal phase space are different from those needed for the linear collider. Thus, the FEL beam must be generated in a different electron source and compressed with additional bunch compressors. The only component of the linear collider that is reused is roughly 5% of the linac which is at most a small fraction of the facility costs for either the linear collider or the X-ray FEL. This is true for all of the linear-collider designs being considered.

If an FEL capability becomes desirable, it can easily be integrated into the NLC complex. The S-band and X-band linacs in the NLC can be used to manipulate the longitudinal phase space so that the beams can be compressed to the very small bunch lengths that are required. Furthermore, the transverse dynamics in the linacs are not an issue because the bunch length is shorter and the vertical emittance for the FEL is much larger than for collider operation.

Possible operational scenarios:

- Introduce an additional S-band linac at the end of the prelinac and add a new bunch compressor. This becomes very similar to the LCLS design. It shares much of the NLC infrastructure.
- Add a parallel X-band linac adjacent to the main linac and run the injector linacs at a higher repetition rate.
- Use the main X-band linac in dedicated FEL operational mode. This reduces the luminosity delivered for high-energy physics or requires operating the low-energy portion of the collider at a higher rate.

Each of these schemes would be very similar through the beginning of the second bunch compressor. The first scenario could be designed as nearly a straightforward copy of the LCLS. Since the S-band injector linacs have relatively long filling times, the FEL beam could be accelerated on the trailing edge of the rf pulses. At the end of the prelinacs, it would then be injected into a dedicated linac for the FEL. The second and third scenarios are similar in that the injector linacs would accelerate the FEL beam through the second bunch compressor. At this point, the FEL beam would be injected into a dedicated FEL X-band linac, which is only a few-hundred meters in length. The last scenario is distinct in that it would use the main X-band linac operating either at a higher repetition rate or with reduced rate to the high-energy IP. These three options are illustrated schematically in Fig. 2.2.

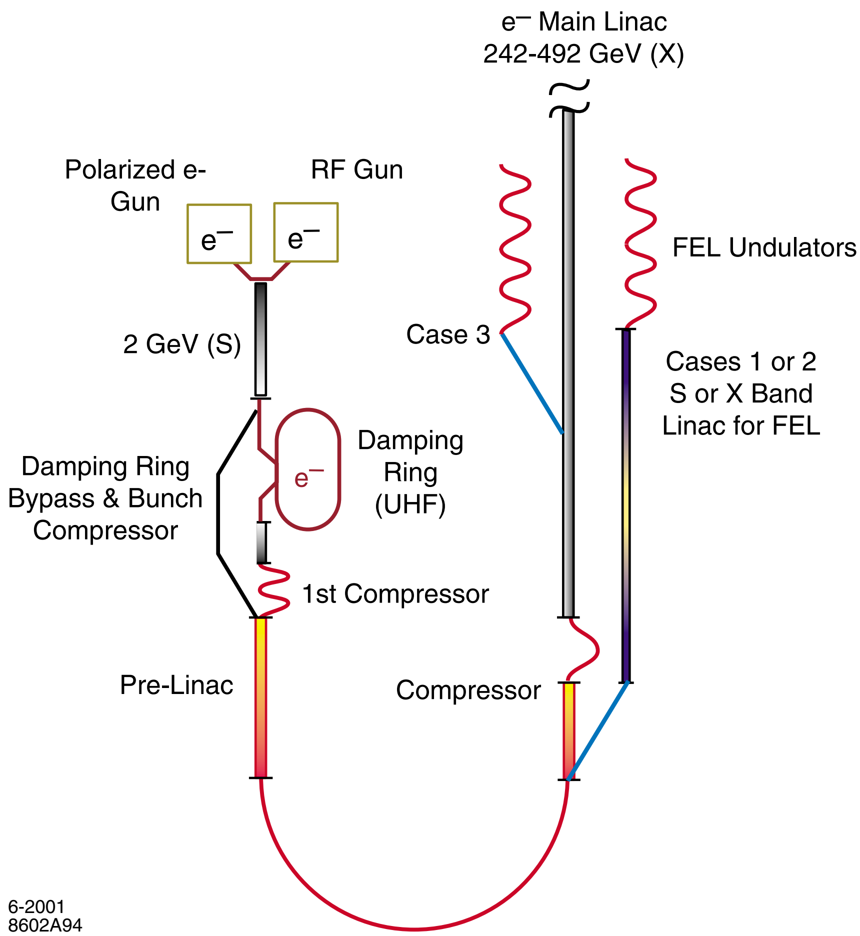

Figure 2.2: Schematic showing the layout of the FEL accelerator sections for three different scenarios.

2.5 Route to a Multi-TeV Linear Collider

The collider described in this report is designed to operate with center-of-mass energies up to 1 TeV or possibly 1.5 TeV. The next logical step for electron-positron facilities would then be a linear collider that operates in the 3- to 5-TeV center-of-mass range with a luminosity of 10^{35} cm^{-2}s^{-1} or more. Some of the technological issues of such a facility, and the parameters which would be required to achieve its goals, have been considered [10,11]. The principal issues that must be addressed are achieving the desired energy and the desired luminosity.

2.5.1 Energy and Accelerating Gradient

Attaining the desired collision energy at a reasonable cost is probably the most difficult issue. The most straightforward route to higher energy – expanding the length of the linacs while using the baseline NLC technology – would require 60 km per linac for 5-TeV cms. Under almost any assumptions, a linear collider with 120 km of total linac length does not seem to be feasible. While the length of the linacs can be reduced by increasing the accelerating gradient, the achievable gradient is not the sole parameter which determines the system cost. For example, doubling the gradient in the NLC structures would require a four-fold increase in rf power. This in turn would require a four-fold increase in rf power components, site-power usage, etc. Although the linac length would be reduced by the increased gradient, the total costs would still be prohibitive. Thus, a multi-TeV linear collider requires both a higher gradient, to limit the linac length and costs associated with length, and a more cost-effective rf power system, to limit the costs that are nominally proportional to the accelerating gradient.

The present limit on achievable accelerating gradient is set by structure damage that is caused by rf breakdowns at high power. The fundamental limits on gradient are known to be higher than the gradients at which damage is observed in prototype multicell structures. For example, the present gradient limit on NLC-type structures is at approximately 70 MV/m, but single cells at the same frequency have operated reliably at gradients of 150-200 MV/m. In Chapter 4 the extensive R&D program on this issue now being carried out by the NLC, KEK and CLIC groups is discussed. The high gradients tolerated by single-cell cavities suggest that a solution to this problem will be found, although the resulting accelerator structures will likely be significantly different from those designed for use in the NLC.

A number of approaches have been suggested that would reduce the cost of the rf system for a future linear collider. These include multibeam klystrons and active pulse compression, both of which are areas of vigorous research. A very promising approach is the two-beam accelerator (TBA) concept used in the CLIC design, in which a low-energy, high-charge drive beam is decelerated in a beamline full of low-impedance rf structures, and the power extracted is used to accelerate a high-energy, low-charge main beam in a series of high-impedance structures. This approach has been studied for some time, and at present appears to be the most likely route to an improved rf power system. A major test facility for both TBA and high-gradient studies at frequencies above X-band will be the CLIC Test Facility 3 (CTF3), which should be operational by 2004 [12].

2.5.2 Luminosity

Table 2.5 lists luminosity-related parameters for TESLA at 0.5-TeV cms, NLC at 1.0-TeV cms, and CLIC at 3.0-TeV cms. The CLIC design's most challenging parameters – beam power, vertical emittance, and vertical rms beam size at the IP – are all reasonable extrapolations from the NLC parameters. The vertical beam size and emittance are reduced by a factor of a few times. This implies that the alignment and jitter tolerances will be somewhat tighter, diagnostic equipment such as BPMs and laser-based profile monitors will require modest improvements, and a small number of additional magnets will require active stabilization. The horizontal beam size and emittance have been reduced by similar factors, implying that an improved damping ring, redesigned bunch compressors, and reduced bending in the beam delivery system will be required to achieve and preserve the small horizontal emittance.

The most significant differences between the NLC and CLIC parameters are related to the beam-beam interaction. The very-high beam energy causes the beamstrahlung energy spread to increase to over 30% and the number of coherent pairs produced is comparable to the number of beam particles. In order to accommodate these larger background sources, the 3-TeV cms linear collider requires a crossing angle of at least 20 mrad [13]. Such a crossing angle appears to be acceptable at higher energies as well. It should be noted that the beamstrahlung is a measure of the fraction of the luminosity far from the nominal center-of-mass energy. The fraction of luminosity close to the nominal energy does not change nearly as much although it does tend to decrease with increasing energy.

2.5.3 The NLC Configuration and Multi-TeV Options

While it is too early to determine the technologies that will be used at a multi-TeV linear collider, a general review of the issues discussed above reveals many of the requirements of such a facility. The NLC configuration has been developed with these requirements in mind. For example, the multi-TeV linear collider will require a site with low levels of ground motion, a crossing angle of at least 20 mrad, beam delivery systems with weak bend magnets, and in all probability a main-linac tunnel that can accommodate a second beamline for the 'drive beam.' All of these features are included in the NLC design. In many cases, the NLC requirements are identical to those of a future facility. In other cases, configuring the NLC design to accommodate a future linear collider incurred no financial or technical penalties. This permits the NLC injectors, beam delivery systems, and main-linac housings to be used in a multi-TeV collider, although the main-linac accelerator structures and rf power sources would need to be replaced. Some upgrades of the damping rings, bunch compressors, and final-focus beamlines would also be required.

Table 2.5: Key parameters for the TESLA, NLC, and CLIC designs

PARAMETER NAME	TESLA	NLC	CLIC
Energy	500 GeV	1 TeV	3 TeV
Luminosity	3.4×10^{34} cm^{-2}s^{-1}	3.4×10^{34} cm^{-2}s^{-1}	10×10^{34} cm^{-2}s^{-1}
Lum. within 1% of E_{cms}	1.7×10^{34} cm^{-2}s^{-1}	1.5×10^{34} cm^{-2}s^{-1}	3.0×10^{34} cm^{-2}s^{-1}
Beamstrahlung	3.2%	10.2%	31%
Bunch Length	300 μm	100 μm	30 μm
Beam Emittance	10×0.02 mm-mrad	3×0.02 mm-mrad	0.7×0.02 mm-mrad
IP Spot Size	553×5 nm	190×2.1 nm	43×1 nm
Beam Power	11.3 MW	13.7 MW	14.8 MW
Rf systems	Super Conducting	Normal Conducting	Normal Conducting
Peak Rf Power	0.2 MW / structure	170 MW / structure	230 MW / structure
Repetition Rate	5 Hz	120 Hz	100 Hz
Bunch train length	950 μs	265 ns	100 ns
Linac tunnel length	30 km	26 km	27 km

The history of accelerator laboratories makes one point clear: the investment in the infrastructure of the accelerators, including the beamline housings, is significant and therefore the infrastructure should be used and reused for as long as possible. This has led to the use of existing synchrotrons as injectors for new synchrotrons, and in some cases to the decommissioning of existing accelerators so that the tunnels or components can be recycled for use in new accelerators. It is this history that has shaped the decision to make the NLC design as compatible as possible with future energy upgrades.

References

[1] American Collider Working Group, *Linear Collider Physics Resource Book for Snowmass 2001*, BNL-52627, CLNS 01/1729, Fermilab-Pub-01/058-E, LBNL-47813, SLAC-R-570, UCRL-ID-143810-DR, LC-REV-2001-074-US.

[2] NLC Design Group, *A Zeroth-Order Design for the Next Linear Collider*, SLAC–474, LBL–PUB–5424, LBNL–PUB–5424, UCRL–ID–124161 (1996).

[3] Adolphsen, C., et al., *Phys. Res. Lett.*, **74**, 2475 (1995).

[4] Raimondi, P. and Seryi, A., “A novel final focus design for future linear colliders,” *Phys. Rev. Lett.*, **86**, 3779 (2001).

[5] Hendrickson, L., et al., “Luminosity optimization feedback in the SLC,” *Proc. Int. Conf. on Acc. and Large Experimental Physics Control Systems* (ICALEPCS 97), Beijing, China (1997).

[6] *2nd International Workshop On High Energy Photon Colliders,* Batavia, Illinois, March 2001, URL: http://diablo.phys.nwu.edu/ggws/.

[7] “3rd International Workshop On Electron-Electron Interactions At TeV Energies”, Santa Cruz, California, December 1999, *Int. J. Mod. Phys*. **A15** 2000.

[8] *Workshop on 4th Generation Light Sources*, Stanford, California, February 1992.

[9] Cornacchia, M., “SASE based 4th generation light sources and the LCLS project,” *Proc. of the 1999 IEEE Part. Acc. Conf.,* New York 1999.

[10] Assmann R. W., et al., “A 3-TeV e+ e linear collider based on CLIC technology,” CERN-2000-008, 2000.

[11] Chen, P., et al., “A 5 TeV Linear Collider on the NLC Site,” *Proc. of the 1996 DPF/DPB Snowmass Meeting*, Snowmass, Colorado 1996.

[12] Braun, H. H., “Achievements and future plans of CLIC test facilities,” *Proc. 18th Int. Conf. on High Energy Acc.,* Tsukuba, Japan, 2001.

[13] Schulte, D., “Machine-Detector Interface for CLIC,” *Proc. of the 2000 Int. Linear Collider Workshop*, Batavia, Illinois 2000.